# Formation and Collimation of Jets by Magnetic Forces

Shibata, K.[1] and Kudoh, T. [2] ; [1]Kyoto University, Japan, [2]NAO, Japan
Email (WC): shibata@kwasan.kyoto-u.ac.jp

**Abstract**

Recent development of theory and numerical simulations of magnetically driven jets from young stellar objects is reviewed. Topics to be discussed are:

1) Acceleration of jets: Magnetically driven jets are accelerated by both magneto-centrifugal force and magnetic pressure force. The former (latter) becomes important when magnetic field is strong (weak). The basic properties (i.e., terminal velocity and mass flux) of jets accelerated by these two forces is discussed in detail. We also discuss the condition of production of jets, which is applied to answer the following question: When do jets begin to be accelerated in the course of star formation ?

2) Collimation of jets: Magnetically driven jets can in principle be collimated by pinching effect of toroidal magnetic fields. Recently, some controvertial arguments have been put forward: Are all field lines (and jets) really collimated by pinching effect ? The current status of this issue is discussed.

3) Protostellar flares: Based on theory and numerical simulations, it has recently been recognized that the formation of jets has a close connection with occurrence of flares (possibly due to magnetic reconnection). We discuss how and when magnetic reconnection occurs in relation to jets.

## 1 Introduction

Magnetically driven jets from accretion disks (Fig. 1) were first proposed to explain jets from active galactic nuclei (Blandford 1976, Lovelace 1976, Blandford and Payne 1982). After the discovery of CO molecular bipolar flow in star forming regions (Snell et al. 1976), the MHD jet model began to be appllied to bipolar flows and jets from young stars (Pudritz and Norman 1986, Uchida and Shibata 1985). The first time-dependent numerical simulation of MHD jets from accretion disks were carried out by Uchida and Shibata (1985) and Shibata and Uchida (1986, 1990; see Fig. 2).

The MHD jet model (see Tsinganos 1996, Tajima and Shibata 1997 for a review) has the following merits: 1) the magnetic force not only *accelerate* plasmas from disk surface to form bipolar jets but also *extract angular momentum* from accretion disks, enabling efficient accretion of plasma onto central objects (stars or black holes), 2) the magnetic force due to toroidal fields *collimate* jets by pinching effect.

It was first thought that molecular outflows were directly ejected from accretion disks (Uchida and Shibata 1985, Pudritz and Norman 1986), but subsequent observations revealed that there exist high velocity neutral winds between molecular outflows and central regions, suggesting that molecular outflows are accelerated by high velocity neutral winds. Hence it is now better to say that the MHD model of jets should be applied to high velocity neutral winds (and also to optical jets).

There are several indirect observational evidence of MHD jets.

(1) Strong magnetic fields are observed in molecular clouds (e.g., Tamura 1999) and T Tauri stars (e.g., Montmerle 1999); $p < B^2/8\pi < \rho GM/r$.

(2) Radiation pressure is not sufficient to drive YSO jets; $\dot{M}V \gg L/c$ (e.g., Lada 1985).

(3) Sometimes helical structures are seen in HH jets, which may correspond to helical magnetic fields (e.g., HH47).

(4) The observation of a spinning outflow was reported (Uchida et al. 1987).

At present, the evidence of a spinning jet is not conclusive (Rodriguez 1999). It would be thus particularly important to detect clear evidence of spinning jets, since the spinning motion of jets is a key physical process to observationally distinguish MHD models and other models. Plasma blobs in non-MHD jets undergo only ballistic motion and cannot rotate around a jet axis.

In this article, we review recent theoretical studies of MHD jets especially on basic physics of acceleration and collimation of jets, rather than discussing detailed intepretation of recent observations. We also discuss magnetic reconnection associated with jets, which has recently been recognized as an important physical process associated with jets and is considered to be a promising mechanism to induce protostellar flares.

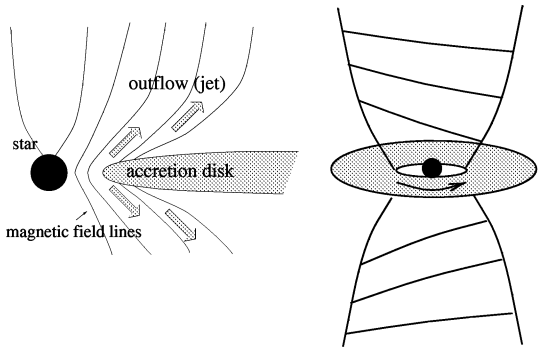


Figure 1: Schematic illustration of magnetically driven jets.

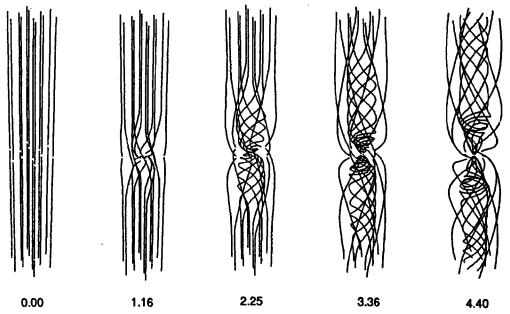


Figure 2: Time dependent MHD simulation of magnetically driven jets ejected from accretion disk (from Shibata and Uchida 1990).

## 2 Acceleration of MHD Jets

### 2.1 When and how a jet is launched ?

Recent nonsteady MHD simulations (Kudoh, Matsumoto, Shibata 1998, Kato, Kudoh, Shibata 1999) have revealed that *even when a jet is highly transient or nonsteady, the Blandford-Payne mechanism (1982) holds; i.e., a jet is launched by the effect of the centrifugal force when the centrifugal force along a rotating field line becomes larger than the gravitational force along the field line.*

Consider the effective gravitational potential

$$\Psi_{eff} = -\frac{1}{2}\Omega^2 r^2 - \frac{GM}{R} \qquad (1)$$

on a rigidly rotating straight magnetic field line with angular velocity $\Omega$ whose footpoint is at a distance $r_0$ from the central mass (Fig. 3). Here $r$ is the distance from the rotation axis of the disk, $R = (r^2 + z^2)^{1/2}$ is the radial distance from the central mass at the origin, and $z$ is the height from the disk plane. The angle between the field line and the disk equatorial plane is $\theta$. Then from the condition $\frac{\partial \Psi_{eff}}{\partial s} < 0$ (centrifugal force > gravitational force) at $(r_0 + \delta r, \delta z)$ and $\delta s = (\delta r^2 + \delta z^2)^{1/2}$, we obtain the following condition

$$\tan^2\theta < 3 + \frac{r_0}{\delta r}\left(\frac{\Omega^2}{\Omega_k^2} - 1\right), \qquad (2)$$

where $\Omega_k = (GM/r_0^3)^{1/2}$ is the Keplerian angular velocity. This equation means that if a disk is the Keplerian disk, the

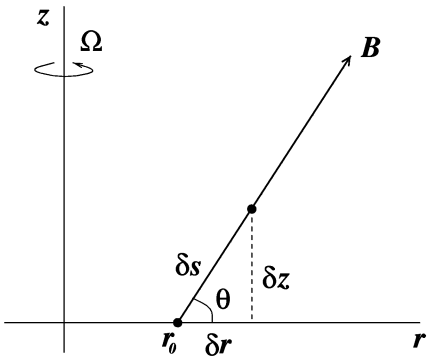


Figure 3: Schematic illustration of the magnetic field configuration near the footpoint of MHD jets.

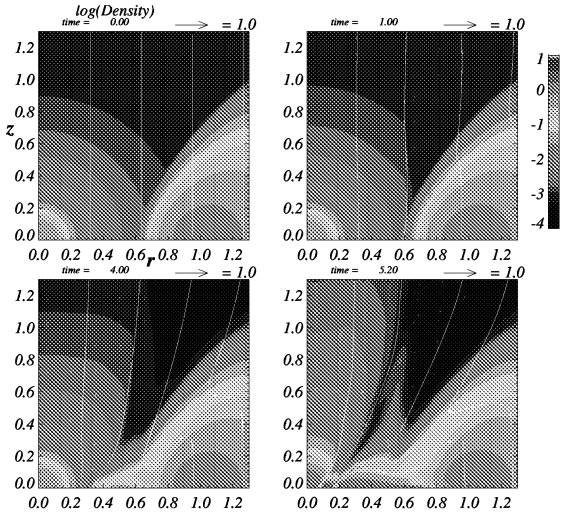


Figure 4: Typical example of MHD jets from a thick disk (Kudoh et al. 1998). The parameters are $E_{mg} = 5 \times 10^{-4}, E_{th} = 0.05$.

critical angle of launching a jet from the (cold) disk is 60° (i.e., Blandford-Payne angle), and that if the disk rotation is sub-Keplerian ($\Omega < \Omega_k$, such as the collapsing disk in the runaway collapsing phase), it is hard to launch a jet from near the disk plane (i.e., small $\delta r = \delta z / tan\theta$). Hence this equation predicts that *a jet is launched after the disk settles into a rotationally supported Keplerian disk (i.e., at the beginning of accretion phase)*, as shown in a very nice numerical simulation of Tomisaka (1998).

As discussed above, it has been found that the Blandford-Payne mechanism is a universal mechanism for launching jets. However, this does not mean that the centrifugal force is a dominant force to accelerate MHD jets. Kudoh and Shibata (1997a) revealed that *for weak magnetic field* ($E_{mg} = (V_A/V_k)^2 < 10^{-2}$), *the magnetic pressure is a dominant acceleration force, while for strong magnetic field* ($E_{mg} > 10^{-2}$), *the (magneto-)centrifugal force is dominant.*

### 2.2 What is a terminal speed of MHD jets ?

The previous 2.5D MHD numerical simulations (Shibata and Uchida 1986, 1990, Stone and Norman 1994, Matsumoto et al. 1996, Hirose et al. 1997, Kudoh et al. 1998, Kato et al. 1999, Kuwabara et al. 1999) and also 3D MHD simulations (Matsumoto and Shibata 1997) have shown that *the velocity of MHD jets is of order of Keplerian velocity at the footpoint*

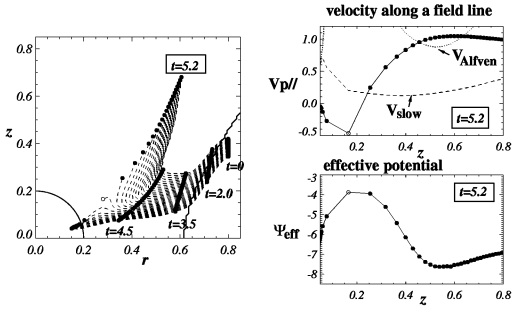


Figure 5: Trajectories of test particles for the case shown in Fig. 4 (Kudoh et al. 1998). Note that fluid particles are accelerated above the local maximum of the effective gravitational (*Blandford-Payne*) potential (eq. 1). This local maximum corresponds to *slow magnetosonic point.*

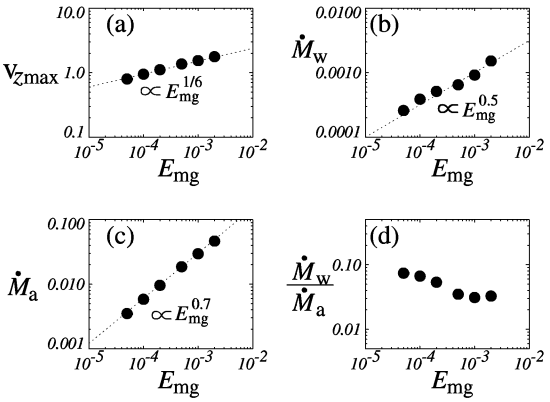


Figure 6: (a) Maximum velocity of jets in unit of Keplerian velocity at the footpoint of jets. (b) Mass flux of jets. (c) Mass accretion rate. (d) Ratio of mass flux of jets to mass accretion rate. All data are based on 2.5D nonsteady MHD simulations in the case of thick disks (Kudoh et al. 1998)

*of MHD jets* and has a weak dependence on $B$ (see Fig. 6);

$$V_{jet} \propto {E_{mg}}^{1/6} \propto B^{1/3}. \tag{3}$$

This is consistent with the results of one-dimensional steady jet theory (Kudoh and Shibata 1995, 1997a; see also Fig. 7), and also can be derived semi-analytically as follows: Since the MHD jet is accelerated by magnetic energy, the kinetic energy of the jet ($\rho V_\infty^2/2$) is comparable to the magnetic energy of the jet ($B_\varphi^2/8\pi$) at infinity (exactly speaking, at the *fast magnetosonic point*). Hence the terminal speed is of order of

$$V_\infty = B_\varphi/(4\pi\rho)^{1/2}. \tag{4}$$

From the condition that the plasma flow must be parallel to the magnetic field line in a co-rotating frame (to maintain steady state), we have

$$\frac{V_\infty}{r\Omega} = \frac{B_p}{B_\varphi}. \tag{5}$$

Since the mass flux is $\dot{M} = 4\pi r^2 \rho V_\infty$, we find

$$V_\infty = \left(\frac{\Omega^2 B_p^2 r^4}{\dot{M}}\right)^{1/3}. \tag{6}$$

This was originally derived by Michel (1969) and hence is called the *Michel velocity.*

It is very important to note that the terminal velocity strongly depends on the mass flux $\dot{M}$. Often people assumes

that the mass flux is a free parameter. Though this assumption is mathematically admissible, it is physically implausible. That is, mass flux is not a given parameter but should be determined by other physical quantities at the boundary. In our problem, the mass flux is approximately given by

$$\dot{M} = 4\pi\rho_{slow}V_{slow}r^2$$
$$= 4\pi\rho_{slow}C_s\frac{B_p}{B}r^2, \quad (7)$$

where $\rho_{slow}$ is the mass density at the *slow magnetosonic point*, $V_{slow}$ is the slow magnetosonic speed, $C_s$ is the sound speed, and $B = (B_p^2+B_\varphi^2)^{1/2}$. In a cold disk, the slow magnetosonic point corresponds to the local maximum of the effective gravitational (Blandford-Payne) potential (Fig. 5), and is located near the disk plane ($\rho_{slow}/\rho_0 \sim 0.1$ in our case). For stronger fields ($E_{mg} > 10^{-2}$), the magnetic field lines become straight $B \sim B_p \gg B_\varphi$ so that the mass flux does not depend on $B_p$, but for weaker fields ($E_{mg} < 10^{-2}$), field lines are highly twisted and the azimuthal component becomes dominant $B \sim B_\varphi \gg B_p$ so that the mass flux is in proportion to $B_p$ (Kudoh and Shibata 1995, 1997a). Considering these effects, the terminal speed of the MHD jet becomes

$$\frac{V_\infty}{V_k} \simeq \left(\frac{\rho_{slow}}{\rho_0}\right)^{-1/6} E_{th}^{-1/6}E_{mg}^{1/6}, \quad (8)$$

where

$$E_{th} = \left(\frac{C_s}{V_k}\right)^2 = \frac{\text{thermal energy}}{\text{gravitational energy}}, \quad (9)$$

$$E_{mg} = \left(\frac{V_A}{V_k}\right)^2 = \frac{\text{magnetic energy}}{\text{gravitational energy}}. \quad (10)$$

Since $\rho_{slow}/\rho_0 \sim 0.1$ and $E_{th}/E_{mg} \simeq \beta$ = gas pressure / magnetic pressure $\sim 1-10$ in the disk, we find from this formula that *the terminal speed of the jet is comparable to the Keplerian velocity* for wide range of parameters since the dependence on parameters is weak; $V_\infty \propto B_p^{1/3}$. This explains the results of the previous 2.5D MHD numerical simulations very well.

Figure 7 shows the mass flux and the terminal velocity of jets as a function of $B_p$ in a steady MHD jet (Kudoh and Shibata 1997a):

$$\dot{M} \propto B_p \quad \text{for weak field} \quad (E_{mg} < 10^{-2}), \quad (11a)$$

$$\dot{M} = \text{const.} \quad \text{for strong field} \quad (E_{mg} > 10^{-2}). \quad (11b)$$

We also find that the terminal velocity shows the following dependence

$$V_\infty \propto B_p^{1/3} \quad \text{for weak field} \quad (E_{mg} < 10^{-2}), \quad (12a)$$

$$V_\infty \propto B_p^{2/3} \quad \text{for strong field} \quad (E_{mg} > 10^{-2}). \quad (12b)$$

Note that the former weak field case corresponds to the *magnetic pressure driven jet* and the latter strong field case corresponds to the *centrifugally driven jet*. Even in the case of strong magnetic fields, the velocity of jets cannot increase freely, since there is an upper limit for the magnetic field strength $E_{mg} = 1$. (If the field strength becomes larger than this critical value, the rotation of accretion disks is stopped by the magnetic force and even the accretion of plasmas is inhibited by the strong magnetic force.) Hence there is an upper limit in the velocity of the jet ejected from accretion disks. This is different from the velocity of the jet ejected from stars (e.g., pulsars). For typical parameters of accretion disks (in the case of Fig. 7), this upper limit of the jet velocity is $\sim 7V_k$.

Finally, we should emphasize again that *even if the magnetic field strenth is very weak in accretion disks, the jet velocity is roughly comparable to Keplerian speed ($Vjet \sim 0.1-1.0V_k$ for $E_{mg} \sim 10^{-8}-10^{-2}$)*. The physical reason is that magnetic field lines are highly twisted by the differential rotation of the disk until the local magnetic energy density ($B_\varphi^2/8\pi$) becomes comparable to the rotational energy ($\rho V_k^2/2 \sim \rho GM/r$ gravitational energy) at the surface of the disk. Since the kinetic energy of the jet ($\rho V_{jet}^2/2$) comes from the magnetic energy, it eventually becomes comparable to the gravitational energy ($\rho V_k^2/2$) at the disk surface (i.e., at the slow magnetosonic point). This process is similar to the magnetorotational (Balbus-Hawley) instability in the sense that the magnetic effect becomes eventually important even if the initial magnetic field is very weak.

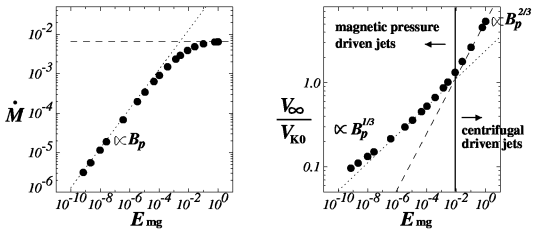


Figure 7: (a) The mass flux of jets, (b) the terminal velocity of jets as a function of magnetic energy $E_{mg} = (V_A/V_k)^2 \propto {B_p}^2$. Note that the critical energy $E_{mg,c}$ separating the *magnetic pressure driven jet* and the *centrifugally driven jet* is about 0.01.

Table 1 Comparison between the magneto-centrifugally driven jet and the magnetic pressure driven jet

| | centrifugal force | magnetic pressure |
|---|---|---|
| poloidal field ($B_p$) | strong | weak |
| field configuration near disk | straight | highly twisted |
| $B_p$ vs $B_\varphi$ | $B_p \gg B_\varphi$ | $B_p \ll B_\varphi$ |
| mass flux ($\dot{M}$) | $\rho C_s r^2$ | $\rho C_s \frac{B_p}{B_\varphi} r^2$ |
| – dependence on $B_p$ | independent of $B_p$ | $\propto B_p$ |
| terminal speed $V_\infty$ | $V_k(\frac{{V_A}^2}{C_s V_k})^{1/3}$ | $V_k(\frac{V_A}{C_s})^{1/3}$ |
| – dependence on $B_p$ | $\propto {B_p}^{2/3}$ | $\propto {B_p}^{1/3}$ |
| range of application | $E_{mg,c} < E_{mg} < 1$ | $E_{mg} < E_{mg,c}$ |

Note: $B_p$ and $B_\varphi$ are the poloidal and toroidal component of magnetic field, respectively, $r$ is the radial distance from the central mass to the footpoint of a jet, $V_k$ is the rotation velocity (Keplerian velocity), $C_s$ is the sound speed, $V_A$ is the poloidal Alfven speed, and $\rho$ is the mass density. These are all measured at the *slow magnetosonic point*. $E_{mg}$ represents the ratio of magnetic energy to gravitational energy at the equatorial plane of the disk, and $E_{mg,c}$ is the critical value separating the *magneto-centrifugally driven jet* and the *magnetic pressure driven jet*, and is $E_{mg,c} \simeq 0.01$ in the case of the model for Fig. 7.

### 2.3 What is a mass accretion rate associated with MHD jets ?

As we discussed in the Introduction, MHD jets play an important role on angular momentum transport from disk to outside, enabling efficient accretion of disk plasma onto a central object. In the case of strong magnetic field ($E_{mg} > 10^{-2}$), the magnetic field play a role of a lever arm which transport angular momentum to the *Alfven radius* $r_A \sim V_\infty/\Omega$. Then the ratio of accretion rate to mass flux of jets (e.g., Pudritz and Norman 1986) becomes

$$\frac{\dot{M}_{acc}}{\dot{M}_{jet}} \sim \left(\frac{r_A}{r_0}\right)^2 \propto {B_p}^{4/3}. \quad (13)$$

On the other hand, in the case of weak magnetic field ($E_{mg} < 10^{-2}$), the lever arm is short so that the local angular momentum transport by magnetic stress becomes more important which is equivalent to the physics of *magnetorotational instability (or Balbus-Hawley (1991) instability)*. In this case,

$$\frac{\dot{M}_{acc}}{\dot{M}_{jet}} \propto {B_p}^a. \quad (14)$$

where $a \sim 0.4-1.0$ (Kudoh et al. 1998). For very weak field strength ($E_{mg} \sim 10^{-4}$), the ratio $\dot{M}_{acc}/\dot{M}_{jet} \sim 10$ (Kudoh et

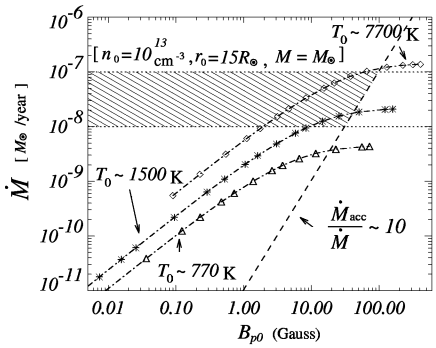


Figure 8: Mass flux of jets as a function of the poloidal magnetic field at the footpoint of the jet. The dashed line shows $\dot{M}_{acc}/\dot{M} \simeq 10$. If $10^{-8} M_\odot/\mathrm{yr} < 10^{-7} M_\odot/\mathrm{yr}$, the wind solution should be within the parameter region that is indicated by a hatched area.

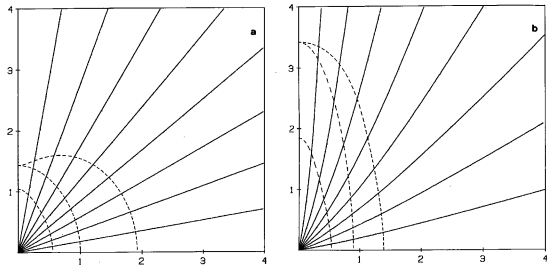


Figure 9: Collimation of the 2D steady MHD wind by self-pinching effect (Sakurai 1985). Left: initial split monopole geometry of magnetic field lines. Right: final poloidal magnetic field configuration (after convergence of steady state solution).

al. 1998). It gradually increases to 100 at around $E_{mg} \sim 10^{-2}$ (Kudoh et al. 1998), and rapidly increases for stronger field $E_{mg} > 10^{-2}$.

### 2.4 Application to YSO jets

When we apply the MHD jet model to YSO (young stellar object) jets, we should first note that the typical values of the basic parameters $E_{th}$ and $E_{mg}$ for YSO jets are

$$E_{th} \simeq 6.5 \times 10^{-4} \left(\frac{T}{10^3\mathrm{K}}\right)\left(\frac{r}{15R_\odot}\right)\left(\frac{M}{1M_\odot}\right)^{-1}, \quad (15)$$

$$E_{mg} \simeq 3.8\times10^{-3} \left(\frac{B}{10\mathrm{G}}\right)^2\left(\frac{n}{10^{13}\mathrm{cm}^{-3}}\right)\left(\frac{r}{15R_\odot}\right)\left(\frac{M}{1M_\odot}\right)^{-1}. \quad (16)$$

Based on these numbers, we find that the jet velocity, mass flux of jets, and mass accretion rate for YSO jets and associated accretion disks (for $a = 1$ in eq. 14) become

$$V_{jet} \simeq 100\ \mathrm{km/s} \left(\frac{B}{10\mathrm{G}}\right)^{1/3}\left(\frac{n}{10^{13}\mathrm{cm}^{-3}}\right)^{-1/6} \times\left(\frac{T}{10^3\mathrm{K}}\right)^{-1/6}\left(\frac{r}{15R_\odot}\right)^{-1/2}\left(\frac{M}{1M_\odot}\right)^{1/2}, \quad (17)$$

$$\dot{M}_{jet} \simeq 10^{-8}\ \mathrm{M}_\odot/\mathrm{yr} \left(\frac{B}{10\mathrm{G}}\right)\left(\frac{n}{10^{13}\mathrm{cm}^{-3}}\right)^{1/2} \times\left(\frac{T}{10^3\mathrm{K}}\right)^{1/2}\left(\frac{r}{15R_\odot}\right)^{5/2}\left(\frac{M}{1M_\odot}\right)^{-1/2}, \quad (18)$$

$$\dot{M}_{acc} \simeq 10^{-6}\ \mathrm{M}_\odot/\mathrm{yr} \left(\frac{B}{10\mathrm{G}}\right)^2\left(\frac{T}{10^3\mathrm{K}}\right)^{-1/2}\left(\frac{r}{15R_\odot}\right)^2. \quad (19)$$

Using these formulae and observed physical quantities of YSO jets (velocity and mass flux), we can predict the physical quantities of accretion disks at the footpoint of the jets. Since the observed velocity of YSO jets is a few 100 km/s and the MHD jet theory predicts $V_{jet} \sim V_k$, the footpoint of the jet must be around $r \sim 15_\odot$. Figure 8 shows the possible relation between the mass flux of jets, the temperature of the disk, and the magnetic field strength at $r = R_\odot$ for solar mass protostars when $n = 10^{13}$ cm$^{-3}$. From this, we can predict that the magnetic field strength at the footpoint of YSO jets is about a few - a few 10 G. We can also see from this figure that the actual YSO jets are intermediate between the *magnetic pressure driven jet* and the *centrifugally driven jet.*

## 3 Collimation of MHD Jets

### 3.1 Can hoop stress collimate jets ?

As the jet propagate farther from the disk, the toroidal component ($B_\varphi$) of magnetic field becomes dominant compared with the poloidal component ($B_p$) (see eq. (5)),

$$\frac{B_\varphi}{B_p} = \frac{r\Omega}{V_\infty} \propto r, \quad (20)$$

since $V_\infty \to$ constant. Thus the pinching force ($B_\varphi^2/(4\pi r)$) becomes important as the jet propagates farther, so that it begins to collimate the jet (Blandford and Payne 1982, Pudritz and Norman 1986, Uchida and Shibata 1985, Shibata and Uchida 1986, Sakurai 1985, 1987, Kaburaki and Itoh 1987, Heyvaerts and Norman 1989, Lovelace et al. 1991, Sauty and Tsinganos 1994, Ouyed and Pudritz 1997, Ustyugova et al. 1999, Bogovalov and Tsinganos 1999). This force is often called the *hoop stress.*

Sakurai (1985) numerically solved the trans-field equation (Grad-Shafranov equation) for the first time and obtained the solution which show logarithmic collimation of field lines to the polar direction: $B_p \sim R^{-2+2\nu}/\log R$ where $0 \le \nu \le 1$ and $R = (r^2 + z^2)^{1/2}$ is the distance from the origin. Heyvaerts and Norman (1989) confirmed the results of Sakurai (1985) using the analytical approach.

While Sakurai (1985)'s results show that the field lines and jet streamlines are actually collimated into the rotation axis of the disk, the collimation is very slow (i.e., it has a logarthmic dependence). The results of the nonsteady 2.5D MHD numerical simulations of the MHD jets from accretion disk also show slow collimation of jet streamlines (Kudoh et al. 1999).

This slow collimation seems to be in contradiction with actual observations, since many jets show strong collimation from near the disk. Hence, some researchers began to consider alternative ideas to explain the apparently collimated jet structure; Spruit et al. (1997) proposed that the *poloidal field* is the main collimating agent. On the other hand, Shu et al. (1995) presented a model in which the *density distribution* show thin jet-like structure, even though actual fluid flows and field lines do not collimate.

### 3.2 Do all magnetic field lines collimate ?

Sakurai (1985)'s numerical calculation showed that all magnetic field lines collimate to polar direction, and Heyvaerts and Norman (1989) analytically confirmed this result. Okamoto (1999), however, presented a different view against this "hoop stress paradigm", and claimed that *all field lines cannot collimate.* He then proposed that the magnetically driven wind consists of two components, *a collimated polar wind* and *an uncollimated equatorial wind.* This argument is based on the $J \times B$ force distribution such that it acts to the polar direction near the pole while it acts to the equatorial plane near the equator. In Sakurai (1985)'s calculation, the current $J$ flowing toward r-direction near the equator is not included since his calculation assumed split monopole field initially. If we initially assume a dipole (similar to the pulsar wind case), the wind tends to be in the equatorial direction near the equator.

In relation to this, Kudoh et al. (1999) examined the collimation of the MHD wind/jet, by using time dependent 2.5D MHD numerical simulations. They studied the production of MHD jets in the case of initially non-uniform magnetic fields, 1) a paraboloidal field, 2) a dipole field produced by a ring current, to see how diverging magnetic field lines are colli-

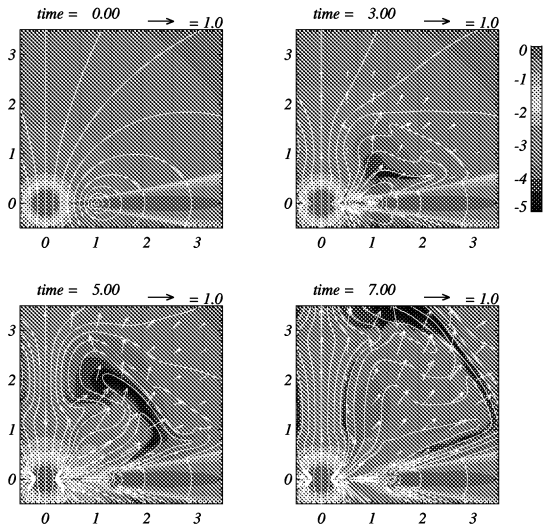


Figure 10: The case when a dipole field produced by a ring current is assumed initially. In this case, not only a collimated polar jet but also an uncollimated equatorial wind are produced (Kudoh et al. 1999).

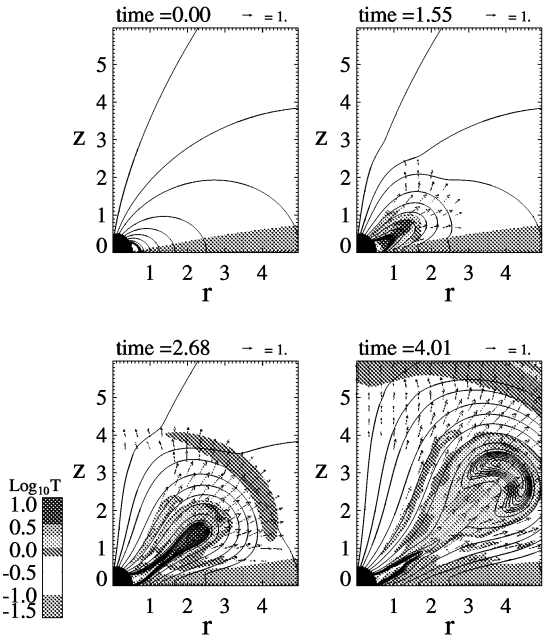


Figure 11: A magnetic reconnection model of protostellar flares (Hayashi et al. 1996). It is assumed that at $t = 0$ a stellar dipole magnetic field penetrates an accretion disk. The parameters in the initial disk (at $r = 1$) are $E_{th} = 2 \times 10^{-3}, E_{mg} = 2 \times 10^{-4}$. The color shows the temperature, and solid curves denote magnetic field lines. The arrows depict velocity vectors in r-z plane.

mated by the hoop stress. In the former paraboloidal case, they found that the jet and field line tend to be collimated by the pinching effect of toroidal fields as the torsional Alfven wave front propagate into the static gas layer (see Kudoh et al. 1999). On the other hand, in the latter dipole case, the magnetically driven outflow consists of not only a collimated polar jet but also an uncollimated equatorial wind (see Fig. 10). This seems to be consistent with Okamoto (1999)'s argument.

In summary, the basic theory of collimation of the MHD jet has not yet been established. Current ideas are controvertial, and more work (both analytical and numerical) will be necessary to settle this important issue.

## 4 Magnetic Reconnection Associated with MHD Jets - Protostellar Flares -

What is occurring in between a protostar and a disk ? Shu et al. (1994) presented a model in which a disk does not have magnetic field and penetrate into stellar magnetosphere through the "X region" (hence this model is called the *X-wind model*), trying to explain angular momentum transport between a star, a disk, and a jet, and also the production of the jet from the "X-region". Though this model has some interesting points, there are a number of uncertainties in this model.

The biggest uncertainty is the presence of the "X-region". This is the most important point of this model, but unfortunately there is no convincing proof (or quantitative calculation) on the existence of such "X-region". Even the word X-region is misleading, since it has no relation to X-point magnetic reconnection. Disk plasmas simply go through the X-region by diffusion process, though the physical origin of such diffusion remained puzzling. It seems that this region was artificially introduced to maintain steady state. The actual state of the region between a star and a disk would be much more dynamic and nonsteady than what the X-wind model assumed (e.g., Hirose et al. 1997; Hayashi et al. 1996). In fact, recent observations of protostars with X-ray satellite ASCA and ROSAT have revealed that protostars are frequently producing supehot flares with temperature of $10^8$ K (Koyama et al. 1996, Montmerle 1999, Tsuboi et al. 1998). Even the jet itself seems to be very nonsteady; knot structures seen in many optical jets (e.g., Burgarella et al. 1993) could be a result of nonsteady production of jets.

Hayashi, Shibata, Matsumoto (1996) presented a magnetic reconnection model of protostellar flares, by performing 2.5D time dependent MHD nummerical simulations of interaction between an accretion disk and stellar magnetosphere (dipole magnetic field). Figure 12 shows one of their simulation models. They assumed that accretion disk plasmas enter the stellar magnetosphere (i.e., accretion disk is penetrated by stellar dipole field at t = 0), and then examined the following evolution of the interaction between a rotating disk and a stellar dipole field. The initial process occurring near the disk is basically the same as those in the nonsteady MHD jet model (e.g., Shibata and Uchida 1986); the disk plasma twists magnetic field and thus generated magnetic twist and associated J x B force (magnetic pressure and centrifugal force) accelerates the plasma in the surface layer of the disk to form an MHD jet from the disk. In this case, the magnetic twist is accumulated in a closed loop, increasing the magnetic pressure of the loop, which eventually leads to the ejection of the magnetic loop after about one orbital period of the disk. After the ejection of the loop, a current sheet is created inside the loop, leading to fast reconnection there. This process is similar to that occurring in solar coronal mass ejections, and basic reconnection mechanism is the same as in solar flares (e.g., Tsuneta et al. 1992, Shibata 1996, Yokoyama and Shibata 1998). The reconnection releases huge amount of magnetic energy of order of $10^{36}$ erg (about $10^4$ times more energetic than solar flares) stored in the sheared loop with a size of $L \sim 10^{11}$ cm. The temperature of super hot plasma created by the reconnection amounts to

$$T \sim 10^8 \left(\frac{B}{100\mathrm{G}}\right)^{6/7} \left(\frac{n_0}{10^9 \mathrm{cm}^{-3}}\right)^{-1/7} \left(\frac{L}{10^{11.5}\mathrm{cm}}\right)^{2/7} \mathrm{K}, \quad (21)$$

which is based on the balance between reconnection heating and conduction cooling (Yokoyama and Shibata 1998, Shibata and Yokoyama 1999). Here $n_0$ is the pre-flare coronal density. These results explain characteristics of protostellar flares observed by ASCA and ROSAT. Hayashi et al. (1996) suggested

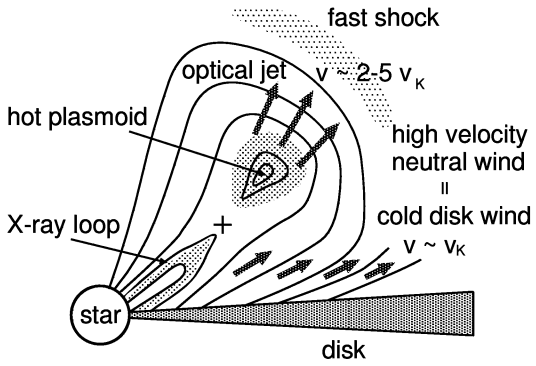


Figure 12: A schematic picture of numerical results by Hayashi et al. (1996). Hot plasma jet ejected from the flaring region corresponds to the optical jet. Cold, dense wind emanating from the disk may explain high-velocity neutral winds.

that the cold jet ejected from the disk and the hot plasmoid ejection may correspond to high speed neutral winds and optical jets, respectively (see Fig. 12).

Similar numerical simulations have been done by Miller and Stone (1997) and Romanova et al. (1998). These simulations revealed that the production of MHD jets are closely related to magnetic reconnection (possibly protostellar flares). Hence it would be interesting to observationally study the relation between protostellar flares and production of jets. (See also Hayashi et al. (1999) on quasi-periodic ejections of plasmoids and associated reconnection with periodicity of about an orbit of the disk.)

Furuya et al. (1999) recently discovered an evidence of a very tiny jet (with a length of order of a few tens AU) by radio interferometric observations. Since the time scale of this jet is a few tens years, there is a high possibility that we can observe both a big flare and an associated MHD jet within a few - 10 years. Hence if big flares occur in some protostars, it would be very interesting to search for jets near such protostars.

## 5 Summary

1) MHD jets are accelerated by both *magnetic pressure* and *(magneto-)centrifugal force*. The magnetic pressure plays dominant role for *weak field* case ($E_{mg} = (V_A/V_k)^2 < 0.01$)), while the centrifugal force is dominant for *strong field* case ($E_{mg} > 0.01$).

2) Mass flux of MHD jets is given by

$$\dot{M} = 4\pi\rho_{slow} C_s \frac{B_p}{B} r^2$$

$$\propto B_p \quad \text{for weak field} \quad (E_{mg} < 10^{-2}),$$
$$= \text{const.} \quad \text{for strong field} \quad (E_{mg} > 10^{-2}).$$

3) The terminal speed of MHD jets is given by the *Michel velocity* and is comparable to Keplerian speed

$$V_\infty = \left(\frac{\Omega^2 B_p^2 r^4}{\dot{M}}\right)^{1/3} = V_k \left(\frac{\rho_{slow}}{\rho_0}\right)^{-1/6} \left(\frac{E_{mg}}{E_{th}}\right)^{1/6}$$

$$\propto B_p^{1/3} \quad \text{for weak field} \quad (E_{mg} < 10^{-2}),$$
$$\propto B_p^{2/3} \quad \text{for strong field} \quad (E_{mg} > 10^{-2}).$$

4) The ejection point of MHD jets is determined by the *Blandford-Payne potential*; a jet begins to be accelerated after the runaway collapse phase is stopped and the accretion phase begins.

5) The hoop stress due to toroidal fields can collimate MHD jets at least around the polar axis.

6) There is a possibility that the entire jet/wind consists of two components: a collimated polar jet and a non-collimated equatorial wind.

7) Magnetic reconnection (possibly, protostellar flares) occurs in close association with production of jets.

**Acknowledgement**

The authors would like to thank Mitsuru Hayashi, Seiichi Kato, and Takuhito Kuwabara for their various help in preparing the authors' talk and manuscript.

**References**

Balbus S. A., Hawley J. F. 1991, ApJ 376, 214
Burgarella D., Livio M., O'Dea C. P. (eds) 1993, *Astrophysical Jets*, Cambridge Univ. Press
Blandford R. D. 1976, MNRAS 176, 465
Blandford R. D., Payne D. G. 1982, MNRAS 199, 883
Bogovalov S., Tsinganos K. 1999, MNRAS 305, 211
Furuya R. et al. 1999, in these proceedings
Hayashi M. R., Shibata K., Matsumoto R. 1996, ApJ 468, L37
Hayashi M. R., Shibata K., Matsumoto R. 1999, in these proceedings
Heyvaerts J., Norman C. 1989, ApJ 347, 1055
Hirose S., Uchida Y., Shibata K., Matsumoto R. 1997, PASJ 49, 193
Kaburaki O., Itoh M. 1987, A&A 172, 191
Kato S., Kudoh T., Shibata K. 1999, in these proceedings
Koyama K. et al. 1996, PASJ 48, L87
Kudoh T., Shibata K. 1995, ApJ 452, L41
Kudoh T., Shibata K. 1997a, ApJ 474, 362
Kudoh T., Shibata K. 1997b, ApJ 476, 632
Kudoh T., Matsumoto R., Shibata K. 1998, ApJ 508, 186
Kudoh T., Matsumoto R., Shibata K. 1999, in these proceedings
Kuwabara T., Kudoh T., Matsumoto R., Shibata K. 1999, in these proceedings
Lada C. J. 1985, ARAA 23, 267
Lovelace R. V. E. 1976, Nature 262, 649
Lovelace R. V. E., Berk H. L., Contopoulos J. 1991, ApJ. 379, 696
Matsumoto R., Uchida Y., Hirose S., Shibata K., Hayashi M. R., Ferrari A, Bodo G., Norman C. 1996, ApJ 461, 115
Matsumoto R., Shibata K. 1997, in Proc. *Accretion Phenomena and Related Outflows*, IAU Colloq. No. 163, PASP Conf. Ser. Vol. 121, Wickramasinghe, D. T. et al. (eds.), p. 443
Michel F. C. 1969, ApJ 158, 727
Miller K. A., Stone J. M. 1997, ApJ 489, 890
Montmerle T. 1999, in these proceedings
Okamoto I. 1999, MNRAS 307, 253
Ouyed R., Pudritz R. E. 1997, ApJ 482, 712
Pudritz R. E., Norman C. 1986, ApJ 301, 571
Romanova M. M., Ustyugova G. L., Koldoba A. V., Chechetkin V. M., Lovelace R. V. E. 1998, ApJ 500, 703
Sakurai T. 1985, A&A 152, 121
Sakurai T. 1987, PASJ 39, 821
Sauty C., Tsinganos K. 1994, A&A 287, 893
Shibata K., Uchida Y. 1986, PASJ 38, 631
Shibata K., Uchida Y. 1990, PASJ 42, 39
Shibata K. 1996, Adv. Space Res. 17, (4/5)9
Shibata K., Yokoyama T. 1999, ApJ Let. in press
Shu F. et al. 1994, ApJ 429, 781
Shu F. et al. 1995, ApJ 455, L155
Snell R. L., Loren R. B., Plambeck R. L. 1980, ApJ 239, L17
Spruit H. C., Foglizzo T., Stehle R. 1997, MNRAS 288, 333
Stone J. M., Norman M. 1994, ApJ 433, 746
Tajima T., Shibata K. 1997, *Plasma Astrophysics*, Addison Wesley
Tamura M. 1999, in these proceedings
Tomisaka K. 1998, ApJ 502, L163
Tsinganos K. (eds.) 1996, *Solar and Astrophysical Magnetohydrodynamic Flows*, Kluwer
Tsuboi Y., Koyama K., Murakami H., Hayashi M., Skinner S., Ueno S. 1998, ApJ 503, 894
Tsuneta S. et al., 1992, PASJ 44, L63
Uchida Y., Shibata K. 1985, PASJ 37, 515
Uchida Y., Kaifu N., Shibata K., Hayashi S. S., Hasegawa T., Hamatake H. 1987, PASJ 39, 907
Ustyugova G. V., Koldoba A. V., Romanova M. M., Chechetkin V. M., Lovelace R. 1999, ApJ 516, 221
Yokoyama T., Shibata K. 1998, ApJ 494, L113